

UDC 546.57:615.275.2

SILVER NANOPARTICLES STABILIZED BY OLIGOMERIC HYPERBRANCHED IONIC LIQUID: STRUCTURE AND ANTIMICROBIAL PROPERTIES**E.A.Lysenkov¹, O.V.Striutskyi², L.P.Klymenko¹, V.V.Shevchenko²**¹*Petro Mohyla Black Sea National University*²*Institute of Macromolecular Chemistry of the National Academy of Sciences of Ukraine**ealysenkov@ukr.net*

Received 23.04.2023

Reviewed 08.08.2023

Accepted 04.09.2023

The peculiarities of the structural organization of silver nanoparticles (AgNP) and their antimicrobial properties were studied using the methods of FTIR spectroscopy, X-ray analysis, electron microscopy and the disc-diffusion method. In this paper, for the first time, an anionic oligomeric ionic liquid with a hyperbranched structure developed by us was used as a surface stabilizer in the synthesis of AgNP. The synthesis of AgNP was carried out by reducing Ag ions in AgNO₃ with trisodium citrate in the presence of this ionic liquid. It was established that there are adsorbed ionic and carbonyl groups on the surface of the formed AgNP, and the formation of complexes between the ionic liquid and silver ions was revealed. According to electron microscopy, the size of the synthesized nanoparticles varies from 8 to 22 nm, with an average value of 14.2 nm. The synthesized silver nanoparticles showed a very high antimicrobial activity against *C. albicans* fungi, while the width of the inhibition zone (d) was 34 mm. In addition, the powder of AgNP shows a very high activity against gram-positive bacteria *S. aureus* (d = 30 mm) and gram-negative bacteria *E. coli* (d = 10 mm).

Keywords: *silver nanoparticles, oligomeric ionic liquid, antimicrobial properties, X-ray structural analysis, electron microscopy.*

doi.org/10.32737/0005-2531-2024-60-69

Introduction

Today, significant efforts of scientists are directed to the creation and research of various nanomaterials due to their unique properties [1]. This nanotechnological approach is widely used in medicine, pharmacy and biology, where the problem of combating pathogenic microorganisms and antibiotic resistance is acute [2]. To solve these problems, silver nanoparticles (AgNP) are widely used, which deserve special attention due to their antimicrobial properties, anti-inflammatory effect and wound healing ability [3].

In addition to bactericidal action, AgNP have unique optical, electrical, dielectric, mechanical, and thermophysical properties [4]. These properties of AgNP significantly depend on their shape, aspect ratio, size and nature of their spatial distribution [5]. It is worth noting that today there are many methods of synthesizing nanoparticles of adjustable size, but the problem of controlling their spatial distribution, i.e. stabilizing their surface to prevent further aggregation, remains unsolved [6–9].

Various chemical, photochemical, physical and biological methods of synthesis [6] using various stabilizers are used to create stabilized AgNP. One of these approaches is the stabilization of AgNP with the help of polymeric macromolecules, for example, polyvinylpyrrolidone (PVP) [7]. PVP contains both a highly polar amide group in the pyrrolidone ring and a nonpolar alkyl skeleton, so it is well soluble in both water and non-aqueous solvents and can act as a stabilizing agent in the dispersion of colloidal metal nanoparticles [8]. With this method of stabilization, it is possible to obtain nanoparticles with a size of 10–30 nm and high antimicrobial activity against a large number of gram-positive and gram-negative bacteria. At the same time, the width of the zone of inhibition for the AgNP-PVP systems varied from 15 to 20 mm [6]. As an alternative to PVP, polyethylene glycol (PEG) is often used to stabilize silver nanoparticles. In work [9], the authors used chemical and biological methods of synthesis of

AgNP using PEG. It was established that the AgNP stabilized by PEG had sizes of 40-47 nm and demonstrated a high antimicrobial activity. The width of the inhibition zone of different types of bacteria was from 12 to 26 mm.

Another approach is the synthesis and stabilization of nanoparticles in the presence of extracts of natural plants and algae [10, 11]. Using this approach, AgNP with sizes of 10-17 nm and high inhibitory activity against *S. aureus* were synthesized [12].

Among known approaches to solving the problem of nanoparticle stabilization, the use of highly branched, especially hyperbranched oligomers as surface stabilizers is promising [13, 14]. The use of hyperbranched oligomeric derivatives of various generations both as they are, including as copolymers, and in combination with traditional reductants in the preparation of AgNP is described [13-15]. Despite the fact that classical ionic liquids are a favorable environment for the formation of nanoparticles of a given shape and size [16] the information on the use of hyperbranched oligomers with ionic liquid groups in their composition (HB-OIL) as stabilizers of AgNP is very limited.

Therefore, the development of new approaches to the synthesis of stabilized silver nanoparticles with high antimicrobial activity is an urgent task. Therefore, the aim of this work was the synthesis of new silver nanoparticles stabilized with the help of HB-OIL and the study of their structure and antimicrobial properties.

Experimental part

Materials. Cyclic anhydride of 2-sulfo-benzoic acid ("Aldrich" $\geq 95\%$), N-methylimidazole ("Aldrich", 99%), AgNO₃ (Pharm.) and trisodium citrate (C₆H₅O₇Na₃, Pharm.) were used without additional purification; hyperbranched aliphatic oligoester polyol Boltorn®H30 ("Perstorp" Sweden) MM 3500 (the equivalent MM of the oligomer by hydroxyl groups, determined by the acylation method, is 117 g/eq) was purified by reprecipitation from dimethylformamide (DMF) into ether followed by drying in a vacuum (1-3 mmHg) at a temperature of 25-30°C for 6 hours; DMF was distilled at a residual pressure of 1-3

mmHg, and ethanol and diethyl ether were used without distillation.

The HB-OIL HB-([SO₃]-[HMim⁺])₃₂ was obtained according to our previously developed method [17, 18] by exhaustive acylation of oligoester polyol (containing 32 terminal primary hydroxyl groups) with cyclic 2-sulfo-benzoic anhydride and subsequent neutralization of the reaction product with N-methylimidazole.

Synthesis procedure. The synthesis of AgNP was based on the reduction of silver in AgNO₃ with trisodium citrate [19] in the presence of our proposed—HB-OIL HB-([SO₃]-[HMim⁺])₃₂ as their surface stabilizer. 0.044 g (0.000260 eq.) of AgNO₃ in 3 ml of water was added to 1.000 g (0.002340 eq.) of HB-([SO₃]-[HMim⁺])₃₂ in 24 ml of water and the mixture was stirred for 10 min at room temperature. Further 0.268 g (0.001040 eq.) of C₆H₅O₇Na₃ in 11 ml of water was added to the mixture followed by stirring for another 10 min. Next, the temperature of the solution was raised to 100°C and refluxed for 1 hour. At the same time, the color of the solution changed from yellow to brown. The solution was filtered, the water was evaporated at 70-75°C, the product obtained as a brown precipitate was vacuumed at a residual pressure of 1-3 mmHg and a temperature of 75-80°C, washed with ethanol and dried in a vacuum (1-3 mmHg) at 75-80°C. The yield is 0.985 g. The obtained product is a brown powder soluble in water and insoluble in organic solvents.

Methods. FTIR spectra were recorded on a "SENSOR 37" spectrophotometer in the spectral range of 600-4000 cm⁻¹. The obtained samples were studied by wide-angle X-ray diffraction on an XRD-7000 diffractometer (Shimadzu, Japan), using CuK_α radiation ($\lambda=1.54 \text{ \AA}$) and a graphite monochromator. The research was carried out by the method of automatic step-by-step scanning in the mode U=30 kV, I=30 mA in the interval of scattering angles from 3.0 to 80 degrees, the exposure time was 5 s. The morphological features of the obtained AgNP were studied by transmission electron microscopy (TEM) using a PEM-125K microscope. Antimicrobial activity of nanocomposites was studied by the diffusion method in agar on a solid

Müller-Hinton nutrient medium for bacteria, and Sabouraud's medium for candida. Petri dishes with a nutrient medium were seeded with 10 μ L of inoculum of test microorganisms *S. aureus*, *E. coli* and *C. albicans* at the rate of $2 \cdot 10^5$ CFU/ml. Synthesized AgNP weighing 0.1 g and disks with control antibiotics azithromycin and ciprofloxacin were placed on the surface of the nutrient medium seeded with test microorganisms. The cups were incubated for 24 hours at a temperature of 37 °C. The indicator of antimicrobial activity was the presence of a clear microorganism-free zone around the disc of the sample with silver nanoparticles. The larger the zone around the disk corresponded to the higher inhibitory efficiency of the sample. The area on the Petri dish that did not contain antimicrobial drugs served as a control. The experiment was repeated three times.

Results and their discussion

The method of obtaining AgNP proposed in this study is based on the reduction of silver in the presence of HB-OIL to stabilize and modify their surface. It should be noted that in this work, for the first time, an anionic protic HB-OIL was used as a surface stabilizer of AgNP. The last one was represented by the ionic oligomer HB-([SO₃]⁻-[HMim⁺])₃₂ with cationic sulfonate imidazolium ionic groups proposed by us earlier in works [17, 18]. According to [20], the heterocyclic cations, carbonyl and residual hydroxyl groups present in this compound are capable of adsorbing on the surface of AgNP, which stabilizes the surface of the latter and contributes to their formation.

For the reduction of silver, trisodium citrate was used as a "mild" reducing agent, which contributes to the stabilization of the surface of the formed AgNP [21].

Preparation of AgNP was carried out by reduction of silver ions in the composition of AgNO₃ with trisodium citrate in the presence of our proposed HB-([SO₃]⁻-[HMim⁺])₃₂ compound for stabilization and modification of their surface. The ratio of silver ions and HB-OIL ionic groups was 1:9, and the ratio of silver ions and trisodium citrate was 1:4. Synthesized AgNP are

brown water-soluble powders and are characterized by a quantitative yield (see the Experimental part), which indicates the completeness of the oxidation-reduction reactions and the efficiency of adsorption of the stabilizer on their surface. The solubility of the obtained AgNP in water greatly simplifies the methods of introducing them into the composition of functionalized polymer materials and obtaining various highly dispersed systems, including hydrosols, and also ensures the manufacturability of their processing, in particular by the electrospinning method [22].

The structure of the synthesized AgNP was investigated using the FTIR spectroscopy method (Figure 1). In the FTIR spectrum of the AgNP (spectrum 2) in comparison with the original HB-OIL (spectrum 1), there is a significant decrease in the intensity of the absorption band of the C=O valence vibrations of ester group bonds, a shift and change in the intensity of the C–C valence vibration absorption bands (1360–1683 cm⁻¹) and C–H (3000–3100 cm⁻¹) bonds of the aromatic component and valence and combined N⁺-H vibrations (2300–3700 cm⁻¹).

Such changes in the spectrum of AgNP indicate the adsorption of carbonyl groups and imidazolium cations on their surface [23] and the formation of complexes of the "guest-host" type between HB-OIL and silver ions. In addition, there are intense absorption bands at 1418 cm⁻¹ and 1575 cm⁻¹ in the spectrum of AgNP, which are related to symmetric and asymmetric valence vibrations of carboxylate anions of trisodium citrate [24], which partially overlap with such valence vibrations of C-C bonds of the aromatic component and deformational vibrations of C-H bonds of methyl and methylene groups of HB-OIL. This indicates the presence of trisodium citrate adsorbed on the surface of the synthesized AgNP and that formed complexes with silver ions. At the same time, adsorbed trisodium citrate in combination with HB-OIL has a stabilizing effect on the surface of the formed colloidal silver particles.

To determine the structure of the obtained nanoparticles, the method of wide-angle X-ray scattering was used.

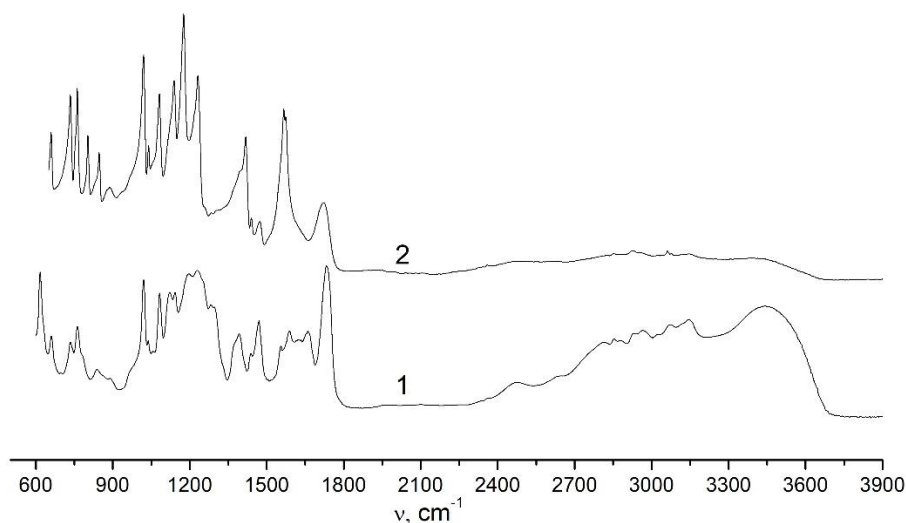


Fig. 1. FTIR-spectra of the original HB-OIL (1) and AgNP (2).

Figure 2 (curve 1) shows the data of X-ray analysis of HB-OIL, which was used to stabilize nanoparticles. This curve is characterized by the presence of a wide halo and the absence of diffraction maxima, which indicates its amorphous structure. To study the reductive ability of HB-OIL and to identify the process of auto-reduction of silver, we obtained diffractograms of model systems that are mixtures of HB-OIL with AgNO_3 obtained at 100°C for 1 hour in water without a reducing agent followed by evaporation (curve 2). This curve is characterized by the presence of an amorphous HB-OIL halo. At the same time, the diffractogram also shows reflexes at 14.0 and 16.8° , which correspond to HB-OIL complexes with silver, a reflex at 44.2° , which indicates the partial formation of a crystal lattice of silver. From the analysis of the obtained curve, it is possible to conclude about the presence of partial recovery of silver in the model system.

Figure 2 (curve 3) shows the X-ray scattering graph for the synthesized powder of silver nanoparticles. A large number of Bragg peaks is observed in the diffractogram. The maxima corresponding to the scattering angles of 26.5 , 29.8 , 36.8 , 43.8 , 46.2 , 54.9 , 64.4 , 77.3° indicate the presence of a crystalline structure in the system silver and correspond to planes (210), (122),

(111), (200), (231), (142), (220), (311), respectively [25]. Therefore, the results of X-ray scattering clearly show that the Ag nanoparticles synthesized according to the method proposed in the paper are crystalline in nature.

It should be noted that the diffractogram contains peaks at 7.3 , 14.6 , 18.3 and 22.2° , which are related to silver citrate [26]. This indicates the presence of citrate anions in the composition of AgNP, which probably form a stabilizing adsorbed layer.

Since the synthesized silver nanoparticles have a crystalline structure, the effective size of the crystallites can be calculated for them using Scherrer equation (1) [27].

$$L = \frac{k\lambda}{\beta \cos \theta_m}, \quad (1)$$

where β is the angular expansion of the diffraction maximum (in radians), which is usually defined as full width at half maximum (FWHM) after preliminary subtraction of background scattering; k – the coefficient depending on the crystallite (if the shape is not known, then $k = 0.9$); θ_m is the angular position of the diffraction maximum. For calculations of the effective size of crystallites for the synthesized particles, we used FWHM, which indicate the crystalline structure of silver (Fig 2, curve 3).

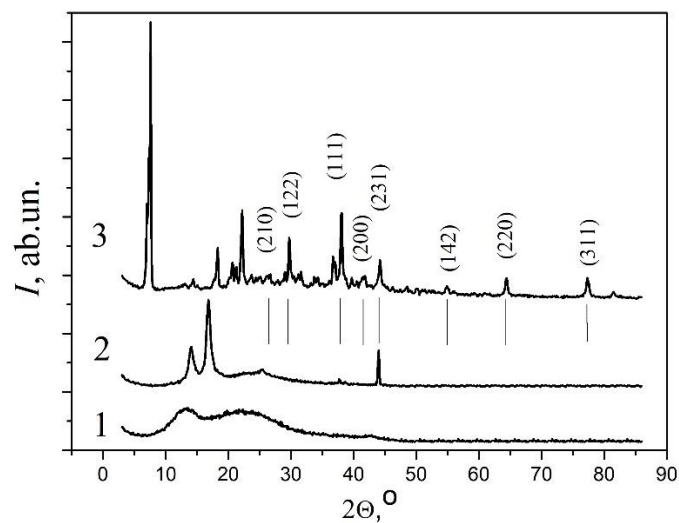


Fig. 2. Diffractogram for OIL (1), mixtures of HB-OIL with AgNO_3 with a ratio of ionic groups and Ag ions equal to 1:9 (2) and silver nanoparticles (3).

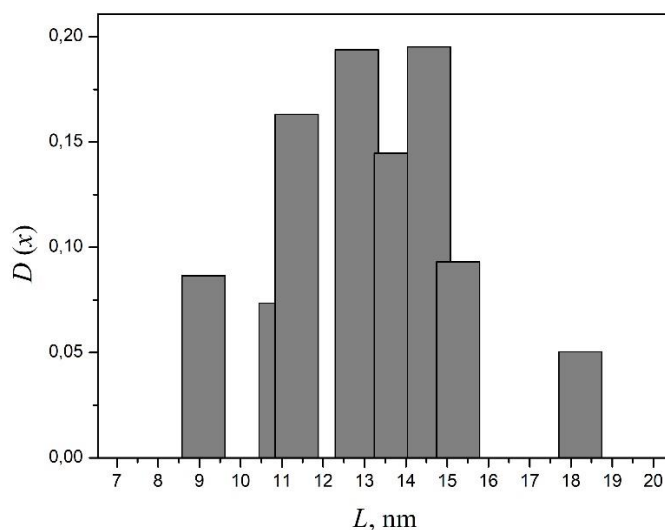


Fig. 3. The size distribution of crystallites obtained from the analysis of X-ray scattering data.

Table 1 shows the values of FWHM, the positions of the maxima, and the crystallite sizes calculated by Eq. (1) for the synthesized silver nanoparticles.

Table 1. Characteristics of maxima and crystallites obtained by Eq. (1)

$2\theta_m, ^\circ$	β, rad	$S, \text{ab.un.}$	L, nm	$D(x)$
26.5	0.0128	625	10.9	0.073
29.8	0.0102	1229	13.7	0.144
36.8	0.0127	1387	11.3	0.163
43.8	0.0101	1659	14.5	0.195
46.2	0.0163	735	9.1	0.086
54.9	0.0120	1648	12.8	0.193
64.4	0.0109	791	14.7	0.093
77.3	0.0096	428	18.2	0.050

The size distribution of crystallites in the studied materials is shown in Figure 3. Figure 3 and the Table 1 show that the size of the crystallites varies from 9 to 18 nm. The most represented fraction of crystalline formations has a size of 12.3 nm.

A more generalized approach for determining the average size of nanocrystalline structures is the Williamson-Hall method [28]. This approach is based on the assumption that both particle size and microdeformation affect the width of the diffraction peak. These two parameters are independent of each other and both are described by the Cauchy-Lorentz distribution. The Williamson-Hall equation has the following form:

$$\beta \cos \theta_m = \frac{k\lambda}{D} + 4\varepsilon \sin \theta_m, \quad (2)$$

where D is the average size of nanocrystalline structures; ε is microdeformation.

To determine D , the parameters obtained from the analysis of crystal peaks were presented as a dependence $\beta \cos \theta_m (4 \sin \theta_m)$, which, according to the Williamson-Hall approach,

should have a linear form. The results of the analysis of crystal peaks are presented on Fig. 3 in the coordinates of Eq. (2).

Figure 4 shows that the dependence $\beta \cos \theta_m (4 \sin \theta_m)$, is linear, which can be described by the equation $y = ax + b$. The results of the approximation are given in Fig. 4 (solid line). Having determined the value of the segment (b) that cuts off the straight line on the Oy axis, you can calculate the average size of silver nanoparticles using the formula:

$$D = \frac{k\lambda}{b}. \quad (3)$$

Using Eq. (3) and the value $b = 0.009$, it was established that the average size of silver nanoparticles is 15.4 nm. This value correlates well with the values of 9–18 nm obtained from the Scherrer equation.

The method of transmission electron microscopy was used to confirm the formation of nanoparticles and study their structural organization.

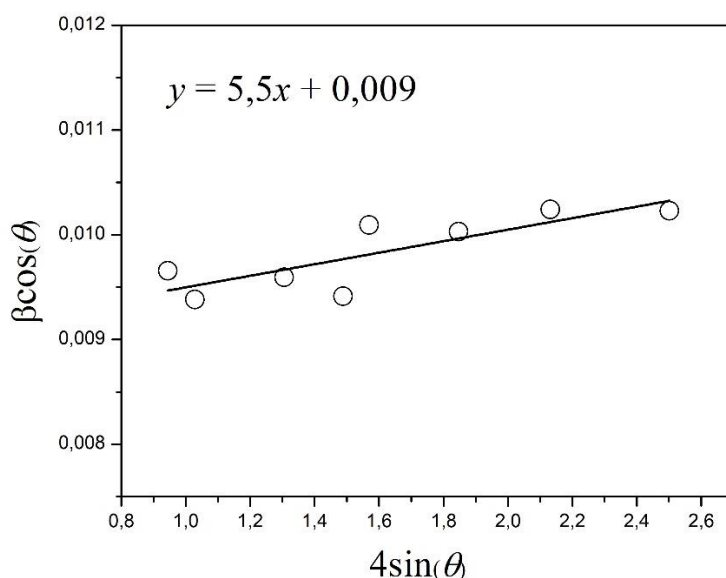


Fig. 4. Dependence $\beta \cos \theta_m$ on $4 \sin \theta_m$ for synthesized silver nanoparticles.

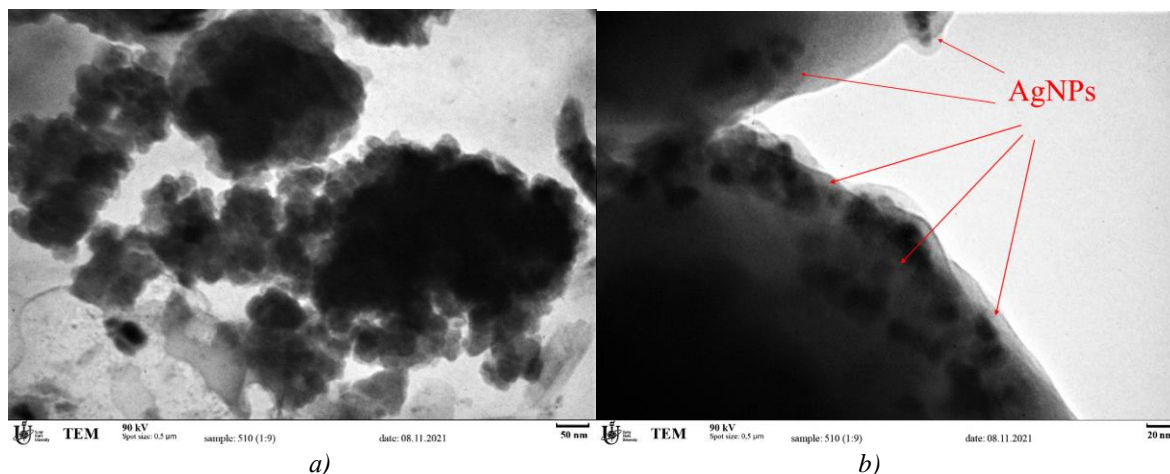


Fig. 5. TEM photographs of synthesized silver nanoparticles in powder form at different magnifications: 40500 (a) and 81000 (b).

Figure 5 shows the structure of powders of the obtained materials at different scale levels. Figure 5a shows that the synthesized poly-dispersed powder consists of small particles that are organized into large aggregates. The size of such aggregates varied from 100 to 300 nm. At a lower scale level (Figure 5b), nanosized particles are observed, which are organized into swarm-like structures.

According to FTIR spectroscopy and X-ray analysis, such nanoparticles are characterized by a core-shell structure, where reduced silver is the core, and HB-OIL in combination with trisodium citrate as a stabilizer forms the shell.

To determine the size of nanoparticles, a series of microphotographs was analysed using

the ImageJ 1.49 v software package. Based on the results of the analysis, a diagram of the distribution of particles by size was constructed (Figure 6).

The particle size varies from 8 to 22 nm, with an average value of 14.2 nm. This average value is very close to the value of $D = 15.4$ nm obtained from the results of X-ray structural analysis.

Figure 6 show that the size distribution of particles has a bimodal character. The maxima in the distribution are observed at sizes of 12 and 16 nm. The position of these maxima is very close to the values obtained during the analysis of diffraction peaks within the Scherrer equation.

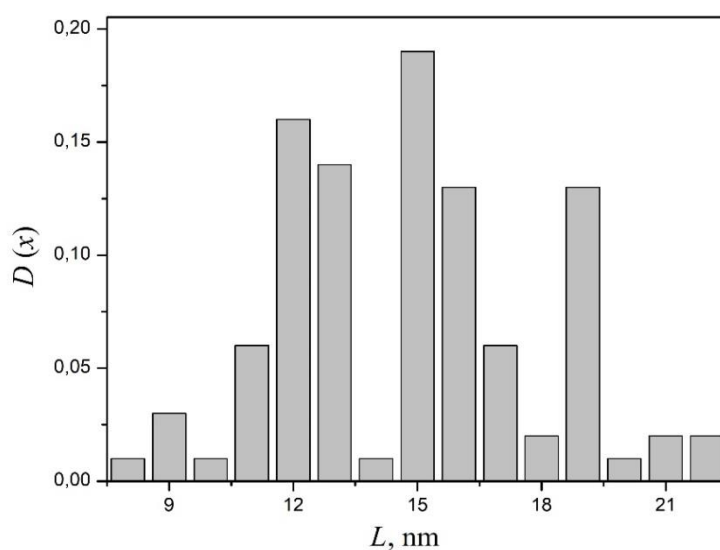


Fig. 6. Size distribution of silver nanoparticles obtained from the results of microphotograph analysis.

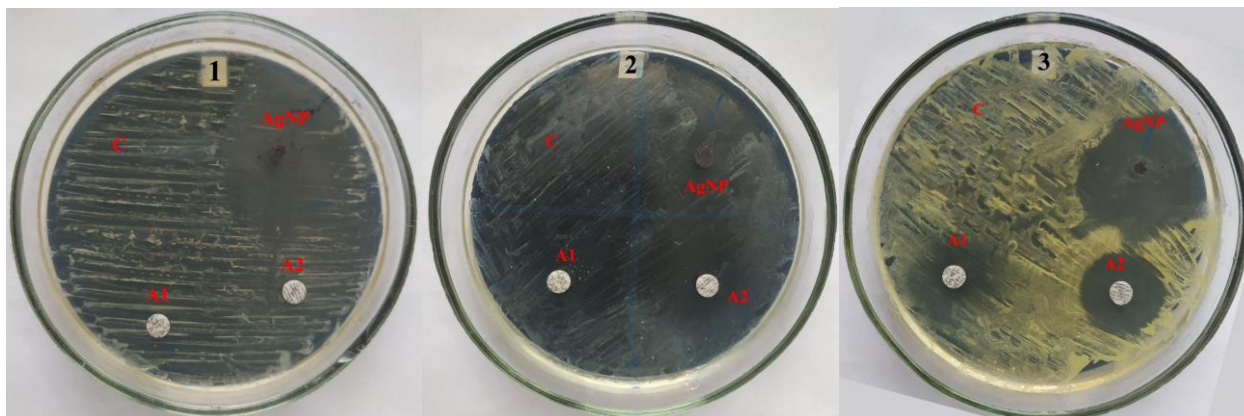


Fig. 7. Antimicrobial activity of AgNP and antibacterial drugs azithromycin (A1) and ciprofloxacin (A2) against *C. albicans* – 1, *S. aureus* – 2, *E. coli* – 3. The letter C indicates the control zone.

Table 2. The value of the width of the inhibition zones for silver nanoparticles and antibacterial drugs.

	<i>S. aureus</i>	<i>E. coli</i>	<i>C. albicans</i>
Ciprofloxacin	20 mm	12 mm	0
Azithromycin	15 mm	8 mm	0
AgNP	30 mm	10 mm	34 mm

Therefore, the results obtained from the data of microscopy and X-ray structural analysis correlate quite well with each other and complement each other.

The next stage of our research was to establish the antimicrobial properties of the synthesized silver nanoparticles. Model bacteria *Staphylococcus aureus* (*S. aureus*) and *Escherichia coli* (*E. coli*), as well as fungi – *Candida albicans* (*C. albicans*) were chosen for analysis. *Staphylococcus aureus* is a gram-positive, *Escherichia coli* is a gram-negative bacteria, and *Candida albicans* is a diploid fungus. To establish the inhibitory activity against microorganisms for the synthesized silver nanoparticles, Petri dishes were seeded with cultures of bacteria and fungi. For the purity of the experiment, a control zone was left on the cups, where microorganisms and classical antibacterial drugs (ciprofloxacin and azithromycin) could freely develop.

Figure 7 shows photos of Petri dishes with various microorganisms. It is shown that the synthesized silver nanoparticles have high antimicrobial activity, which is evidenced by the width of the zone of inhibition (delayed growth of microorganisms). Tab. 2 shows the widths of inhibition zones for silver nanoparticles and classical antibacterial drugs.

Antibacterial drugs showed high antimicrobial activity against gram-positive and gram-negative bacteria, but, as expected, they are neutral against *C. albicans* fungi (Figure 7, Table 2). However, the synthesized silver nanoparticles showed a very high antimicrobial activity relative to these fungi, while the width of the inhibition zone was 34 mm. Also, the AgNP powder shows very high activity against gram-positive bacteria *S. aureus*, while the width of the inhibition zone is 30 mm, which is twice as much as for the antibacterial drug azithromycin. Regarding gram-negative bacteria *E. coli*, silver nanoparticles show similar activity to ciprofloxacin, the width of the zone of inhibition is 10 mm for both materials.

Therefore, synthesized silver nanoparticles have high antimicrobial activity and can be used as components of antiseptic materials.

Conclusions

As a result of the work, new silver nanoparticles stabilized with an hyperbranched oligomeric ionic liquid (HB-OIL) were synthesized and their structure and antimicrobial properties were studied. FTIR spectroscopy data indicate the adsorption of carbonyl and ionic (their cationic component) groups on the surface of the formed AgNP and the formation of "guest-host" type complexes between the ionic

liquid and silver ions. Also, the material contains trisodium citrate adsorbed on the surface of the synthesized AgNP and trisodium citrate that has formed complexes with silver ions. At the same time, trisodium citrate in combination with HB-OIL performs a stabilizing effect in relation to the formed particles of colloidal silver. X-ray scattering results indicate that the silver nanoparticles are crystalline in nature, with crystallite sizes ranging from 9 to 18 nm. The most represented fraction of crystalline formations has a size of 12.3 nm. Using the Williamson-Hall method, it was established that the average size of silver crystallites is 15.4 nm. According to FTIR spectroscopy and X-ray analysis, the synthesized nanoparticles are characterized by a core-shell structure, where reduced silver is the core, and HB-OIL in combination with trisodium citrate as a stabilizer forms the shell. According to electron microscopy, the particle size varies from 8 to 22 nm, with an average value of 14.2 nm. Synthesized silver nanoparticles have high antimicrobial activity against bacteria (*S. aureus*, *E. coli*) and mycotic flora (*C. albicans*). Such nanoparticles can be used as components of antiseptic materials and fillers for developing antimicrobial polymer nanocomposite coatings.

Acknowledgement

This study was funded from the State Budget of Ukraine within the framework of the scientific project No. 0122U002326 “Development of innovative technologies for the creation of the newest silver-containing antimicrobial nanocomposite polymers materials with specified multi-functional special purpose characteristics” commissioned by the Ministry of Education and Science of Ukraine

References

- Baig N., Kammakam I., Falath W. Nanomaterials: a review of synthesis methods, properties, recent progress, and challenges. *Mater. Adv.* 2021. V. 2. P. 1821–1871. doi: 10.1039/d0ma00807a.
- Zewde B., Ambaye A., Stubbs J. III, Dharmara R. A Review of Stabilized Silver Nanoparticles – Synthesis, Biological Properties, Characterization, and Potential Areas of Applications. *JSM Nanotechnol Nanomed.* 2016. V. 4, № 2. P. 1043.
- Nqakala Z.B., Sibuyi N.R.S., Fadaka A.O., Meyer M., Onani M.O., Madiehe A.M. Advances in Nanotechnology towards Development of Silver Nanoparticle-Based Wound-Healing Agents. *Int. J. Mol. Sci.* 2021. V. 22, № 20. P. 11272. doi: 10.3390/ijms222011272.
- Zhang X.F., Liu Z.G., Shen W., Gurunathan S. Silver Nanoparticles: Synthesis, Characterization, Properties, Applications, and Therapeutic Approaches. *Int. J. Mol. Sci.* 2016. V. 17, № 9. P. 1534. doi: 10.3390/ijms17091534
- Khodashenas B., Ghorbani H.R. Synthesis of silver nanoparticles with different shapes, *Arabian Journal of Chemistry.* 2019. V. 12, № 8. P. 1823–1838. doi: 10.1016/j.arabjc.2014.12.014
- Natsuki J., Natsuki T., Hashimoto Y. A review of silver nanoparticles: synthesis methods, properties and applications. *Int. J. Mater. Sci. Appl.* 2015. V. 4. P. 325–332. doi: 10.11648/j.ijmsa.20150405.17
- Bhatia D., Mittal A., Malik D.K. Antimicrobial activity of PVP coated silver nanoparticles synthesized by *Lysinibacillus varians*. *3 Biotech.* 2016. V. 6. P. 196. doi: 10.1007/s13205-016-0514-7
- Koczur K.M., Mourdikoudis S., Polavarapu L., Skrabalak S.E. Polyvinylpyrrolidone (PVP) in Nanoparticle Synthesis. *Dalton Trans.* 2015. V. 44. P. 17883–17905. doi: 10.1039/C5DT02964C
- Mohamad Kasim A.S., Ariff A.B., Mohamad R., Wong F.W.F. Interrelations of Synthesis Method, Polyethylene Glycol Coating, Physico-Chemical Characteristics, and Antimicrobial Activity of Silver Nanoparticles. *Nanomaterials.* 2020. V. 10, № 12. P. 2475. doi: 10.3390/nano10122475
- Cavalli P.A., Wanderlind E.H., Hemmer J.V., Gerlach O.M.S., Emmerich A.K., Bella-Cruz A., Tamanahae M., Almerindo G.I. Pterocladia capillacea-stabilized silver nanoparticles as a green approach toward antibacterial biomaterials. *New J. Chem.* 2021. V. 45. P. 3382–3386. doi: 10.1039/D0NJ05150K
- Mohamed J.M.M., Alqahtani A., Kumar T.V.A., Fatease A.A., Alqahtani T., Krishnaraju V., Ahmad F., Mena F., Alamri A., Muthumani R., Rajendran V. Superfast Synthesis of Stabilized Silver Nanoparticles Using Aqueous *Allium sativum* (Garlic) Extract and Isoniazid Hydrazide Conjugates: Molecular Docking and In-Vitro Characterizations. *Molecules.* 2022. V. 27. P. 110. doi: 10.3390/molecules27010110
- da Silva Ferreira V., ConzFerreira M.E., Lima L.M.T.R., Frases S., de Souza W., Sant’Anna C. Green production of microalgae-based silver chloride nanoparticles with antimicrobial activity against pathogenic bacteria. *Enzyme Microb. Technol.* 2017. V. 97. P. 114–121. doi: 10.1016/j.enzmictec.2016.10.018
- Zhao Y., Liu L., Li C. Ye B., Xiong J., Shi X. Immobilization of polyethyleneimine-templated silver nanoparticles onto filter paper for catalytic applications. *Colloids Surf. A Physicochem. Eng.*

- Asp. 2019. V. 571. P. 44–49. doi: 10.1016/j.colsurfa.2019.03.075
14. Bae J., Park H.J., Kim M.-R. Kim I. Dumbbell-type hyperbranched-polyglycidol-assisted green synthesis of metal nanoparticles. *Nanosci. Nanotechnol.* 2017. V. 17, № 10. P. 7373–7380. doi: 10.1166/jnn.2017.14795
 15. Lysenkov E., Stryutsky, O., Polovenko, L. Development of Nanocomposite Antimicrobial Polymeric Materials Containing Silver Nanoparticles. In: *Nanomaterials: Applications and Properties (IEEE NAP 2022)*. Proc. of 12th International Conference "Nanomaterials: Applications and Properties" (11-16 September 2022, Krakow, Poland), doi: 10.1109/NAP55339.2022.9934675.
 16. Husanu E., Chiappe C., Bernardini A., Cappello V., Gemmi M. Synthesis of colloidal Ag nanoparticles with citrate based ionic liquids as reducing and capping agents. *Colloids Surf. A: Physicochem. Eng. Asp.* 2018. V. 538. P. 506–512. doi: 10.1016/j.colsurfa.2017.11.033
 17. Shevchenko V.V., Stryutsky A.V., Klymenko N.S., Gumenna M.A., Fomenko A.A., Bliznyuk V.N., Trachevsky V.V., Davydenko V.V., Tsukruk V.V. Protic and aprotic anionic oligomeric ionic liquids. *Polymer.* 2014. V. 55, № 16. P. 3349–3359. doi: 10.1016/j.polymer.2014.04.020
 18. Xu W., Ledin P.A., Shevchenko V.V., Tsukruk V.V. Architecture, assembly, and emerging applications of branched functional polyelectrolytes and poly(ionic liquid)s. *ACS Appl. Mater. Interfaces.* 2015. V. 7, № 23. P. 12570–12596. doi: 10.1021/acsami.5b01833
 19. Rivas L., Sanchez-Cortes S., Garcia-Ramos J.V., Morcillo G. Growth of silver colloidal particles obtained by citrate reduction to increase the raman enhancement factor. *Langmuir.* 2001. V. 17, № 3. P. 574–577. doi: 10.1021/la001038s
 20. Tian N., Ni X.F., Shen Z.Q. Synthesis of main-chain imidazolium-based hyperbranched polymeric ionic liquids and their application in the stabilization of Ag nanoparticles. *React. Funct. Polym.* 2016. V. 101. P. 39–46. doi: 10.1016/j.reactfunctpolym.2016.02.005
 21. Dawadi S., Katuwal S., Gupta A., Lamichhane U., Thapa R., Jaisi S., Lamichhane G., Bhattarai D.P., Parajuli N. Current research on silver nanoparticles: Synthesis, characterization, and applications. *J. Nanomater.* 2021. V. 2021, Art. ID 6687290. doi: 10.1155/2021/6687290
 22. Zhao D.M., Feng Q.M., Lv L.L., Li J. Fabrication and Characterization of Cellulose Acetate Ultrafine Fiber Containing Silver Nanoparticles by Electrospinning. *Adv. Mat. Res.* 2011. V. 337. P. 116–119. doi: 10.4028/www.scientific.net/amr.337.116
 23. Kumar B., Smita K., Cumbal L., Debut A. Green synthesis of silver nanoparticles using andean blackberry fruit extract. *Saudi J. Biol. Sci.* 2017. V. 24, № 1. P. 45–50. doi: 10.1016/j.sjbs.2015.09.006
 24. Barani H., Mahltig B. Using microwave irradiation to catalyze the in-situ manufacturing of silver nanoparticles on cotton fabric for antibacterial and UV-protective application. *Cellulose.* 2020. V. 27. P. 9105–9121. doi: 10.1007/s 10570-020-03400-6
 25. Meng Y. A Sustainable Approach to Fabricating Ag Nanoparticles/PVA Hybrid Nanofiber and Its Catalytic Activity. *Nanomaterials.* 2015. V. 5. P. 1124–1135. doi:10.3390/nano5021124
 26. Djokic S. Synthesis and Antimicrobial Activity of Silver Citrate Complexes. *Bioinorganic Chemistry and Applications.* 2008. V. 2008, Art. ID 436458. doi:10.1155/2008/436458
 27. Seo D., Yoo C., Chung I.S., Park S.M., Ryu S., Song H. Shape adjustment between multiply twinned and single-crystalline polyhedral gold nanocrystals: decahedra, icosahedra, and truncated tetrahedra. *J. Physical Chemistry C.* 2008. V. 112. № 7. P. 2469–2475. doi: 10.1021/jp 7109498
 28. Mote V.D., Purushotham Y., Dole B.N. Williamson-Hall analysis in estimation of lattice strain in nanometer-sized ZnO particles. *J. Theoretical and Applied Physics.* 2012. V. 6. Art. № 6. doi: 10.1186/2251-7235-6-6

OLİQOMERİK HİPERBUDAQLI İON MAYESİ İLƏ STABİLİZƏ OLUNAN GÜMÜŞ NANOHİSSƏCİKLƏRİ: QURULUŞU VƏ ANTIMİKROB XÜSUSİYYƏTLƏRİ

E.A.Lisenkov, A.V.Stryutski, L.P.Klimenko, V.V.Şevçenko

İQ-spektroskopiya, rentgen difraksiya analizi, elektron mikroskopiya və disk diffuziya metodundan istifadə etməklə gümüş nanohissəciklərin (SNP) struktur təşkilinin xüsusiyyətləri və onların antimikrob xassələri öyrənilmişdir. Bu işdə ilk dəfə olaraq SNP-lərin sintezində səth stabilizatoru kimi tərəfimizdən inkişaf etdirilmiş hiper budaqlı quruluşa malik anion oliqomerik ion mayesindən istifadə etdik. SNP-lər bu ionlu mayenin iştirakı ilə AgNO_3 -də Ag ionlarının trisodiyum sitrat ilə reduksiyası ilə sintez edilmişdir. Müəyyən edilmişdir ki, əmələ gələn SNP-lərin səthində adsorbsiya olunmuş ion və karbonil qrupları yerləşmiş, ion maye ilə gümüş ionları arasında komplekslərin əmələ gəlməsi aşkar edilmişdir. Elektron mikroskopiya görə, sintez edilmiş nanohissəciklərin ölçüsü 8-22 nm arasında dəyişir və orta dəyəri 14.2 nm-dir. Sintez edilmiş gümüş nanohissəciklər *C. albicans* göbələklərinə qarşı çox yüksək inhibə qabiliyyəti göstərmiş, inhibisiyon zonasının eni d isə 34 mm olmuşdur. Həmçinin, SNP tozu qram-müsbət bakteriyalara *S. aureus* (d = 30 mm) və qram-mənfi bakteriyalar *E. coli* (d = 10 mm) qarşı çox yüksək fəaliyyət göstərir.

Açar sözlər: gümüş nanohissəciklər, oliqomerik ion mayeləri, antimikrobiyal xüsusiyyətlər, rentgen şüalarının difraksiya analizi, elektron mikroskopiyası.